Vietnam Journal of Mechanics, VAST, Vol. 43, No. 3 (2021), pp. 265 – 276
DOI: https://doi.org/10.15625/0866-7136/15879

DEVELOPMENT OF A NOVEL MR CLUTCH FEATURING TOOTH-SHAPED DISC

Quoc Hung Nguyen[1,*], Bao Tri Diep[2,3], Duy Hung Nguyen[1], Van Bien Nguyen[3], Van Bo Vu[3], Qui Duyen Do[1]

[1]*Faculty of Engineering, Vietnamese-German University, Binh Duong, Vietnam*
[2]*Faculty of Civil Engineering, HCMC University of Technology and Education, Vietnam*
[3]*Faculty of Mechanical Engineering, Industrial University of Ho Chi Minh City, Vietnam*
[*]E-mail: hung.nq@vgu.edu.vn

Received: 14 February 2021 / Published online: 30 September 2021

Abstract. In this research, we focus on development of a new configuration of magnetorheological fluid (MRF) based clutch (MRC) featuring a tooth-shaped disc with multiple teeth acting as multiple magnetic poles of the clutch. The tooth-shaped disc is placed in a clutch housing composed of the left housing and the right housing. The inner face the housing also has tooth shaped features mating with the teeth of the disc through the working MRF. Excitation coils are placed directly on stationary winding cores placed on both side of the clutch housing. An air gap of 0.3 mm is left between the housing and the winding cores to ensure the housing can freely rotate against the winding cores. After the introductory part, configuration of the MRC is introduced and the transmitted torque of the MRC is derived. An optimization process to minimize the overall volume of the proposed clutch, which can generate a required maximum braking torque, is then conducted. The optimal results show that the overall volume of the proposed MRC is significantly reduced compared to a referenced conventional MRC (0.159 m^3 vs. 0.295 m^3). A prototype of the proposed MRC is fabricated for experimental works and good agreement between the experimental results and simulated ones is archived.

Keywords: magnetorheological fluid (MRF), MR clutch, tooth-shaped rotor, optimal design.

1. INTRODUCTION

Magnetorheological fluid, called MRF for short, is a type of smart fluids, composed of tiny magnetic particles (micro to nanometer size) dispersed in a base (carrier) fluid. In case of nonexistence of magnetic field, the particles are dispersed randomly and MRF rheologically behaves as Newtonian fluid like carrier fluid. In the existence of a magnetic field, the particles are magnetized, which consequently experienced attractive forces, forming chain-like structure. At high field intensity, the MRF is almost solidified. This change is very fast (few milliseconds) and almost reversible. With this especial property,

the MRF is very potential for various applications such as valves, dampers, clutches, brakes and engine mount [1,2].

There have been a number of researches on MRF based clutch (called MR clutch or MRC for short in this paper). In the early stage, most of the researchers proposed the MRC configurations with rotating coils [4–6]. Obviously, this configuration possesses several disadvantages such as difficulties in manufacturing, unsteady and high friction due to brushes, "bottle-neck" problems of magnetic circuits. To overcome the above disadvantages, new configurations with stationary winding housing have been recently implemented. In this new configuration, the coils of MRCs are wounded on a fixed housing, on which the input shaft (usually connected to the disc of the MRC) and the output shaft (usually connected to the housing of the MRC) are assembled as shown in Fig. 1 [3,7,8]. Thanks to this new configuration, the coil is stationary and brushes can be eliminated. Hence, some disadvantages of conventional MRC such as magnetic flux "bottle-neck" problems, unsteady contact of the brushes, manufacturing difficulties, etc. can be handled. In previous researches, the clutch discs have cylindrical shape and the torque is transmitted from the input shaft to the output shaft via the MRF in the ducts at the end-faces and outer cylindrical face of the disc. Therefore, in order to archive large transmitted torque, the disc should have large size, which results in large size of the MRC and high inertia effect.

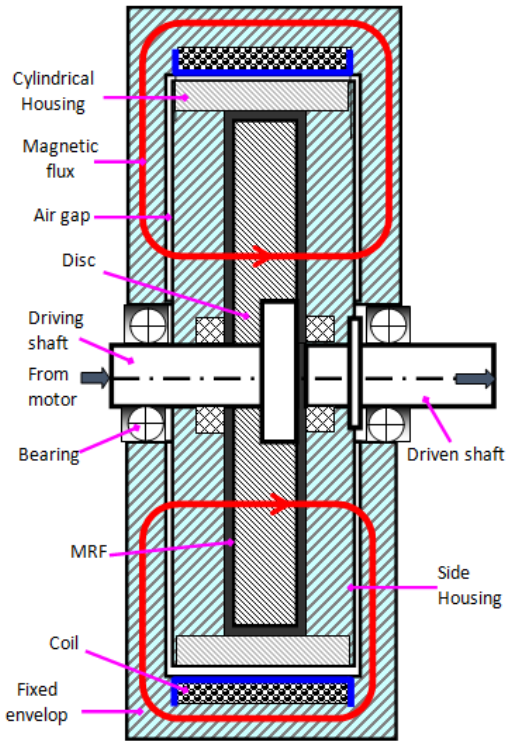

Fig. 1. Configuration of the previous MRC [3]

The main purpose of this study is to develop a compact size MRC featuring a tooth-shaped disc. With the toothed shaped disc, the working area between the disc and the MRF is larger and a high transmitted torque can be archived while size of the MRC is still kept compact.

2. THE MR CLUTCH FEATURING TOOTH-SHAPED ROTOR

The configuration of the proposed MRC with tooth-shaped disc is illustrated in Fig. 2. From the figure, it can be seen that a tooth-shaped disc (made of magnetic material) is fixed to the driving shaft (made of nonmagnetic material). The disc is placed inside housing of the clutch. The inner face of the clutch housing has teeth as well, mating with the teeth of the disc via MRF medium. One side of the clutch housing is connected to the driven shaft (made of nonmagnetic steel). In order to avoid the MRF leaking, a mechanical lip-seal is used. Two ball bearings are used for relative rotation between the

housing (output shaft) and the disc input shaft). Two fixed winding cores, on which the coils are wound, are assembled on both side of the clutch housing. The cores are attached to the corresponding fixed supports, on which the clutch shafts are also assembled. By assembly the cores and the clutch shaft on the support, relative position between the clutch housing and the cores can be assured. To ensure a free rotation of the clutch housing relatively to the winding cores, a small air gap (0.3 mm) between the housing and the winding cores is employed. When a current is applied to coils, an induced magnetic field is created causing the MRF becomes solid-like. By control the applied current, a controllable transmitted torque from the input shaft to the output shaft can be archived.

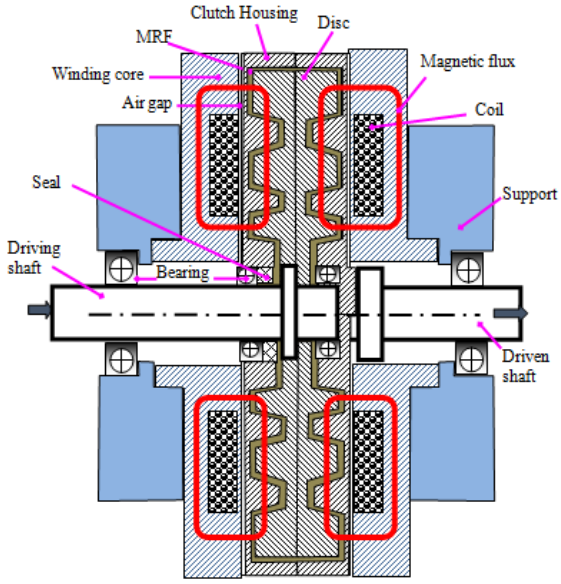

Fig. 2. Configuration of the proposed tooth-shaped mRC

In order to derive transmitted torque of the MRC, firstly a small ring element in an inclined duct of MRF shown in Fig. 3 is analyzed. The friction torque acting to this element can be calculated by

$$\mathrm{d}T = r\tau \mathrm{d}A = 2\pi r^2 \tau \mathrm{d}l = 2\pi \left(R_1 + l\sin\varphi\right)^2 \tau \mathrm{d}l, \tag{1}$$

where r is the radius of the small ring element; R_1 and R_2 are the radii of the first end and the second end of the inclined duct respectively, and L is the length of the inclined duct. By assuming a linear velocity profile of MRF in the duct, the Bingham model of MRF in the duct can be mathematically expressed by

$$\tau = \tau_y + \mu\frac{r\Delta\omega}{d} = \tau_y + \mu\frac{\delta\omega\left(R_1 + l\sin\varphi\right)}{d}, \tag{2}$$

where τ is the tangent shear stress acting on the MRF element; φ is the angle between the inclined duct and the rotational axis; $\delta\omega$ is the relative angular velocity between the

two walls of the duct, which is also the relative angular speed between the disc and the housing); d is the duct gap size; τ_y and μ are in sequence the yield stress and the post-yield viscosity of the MRF.

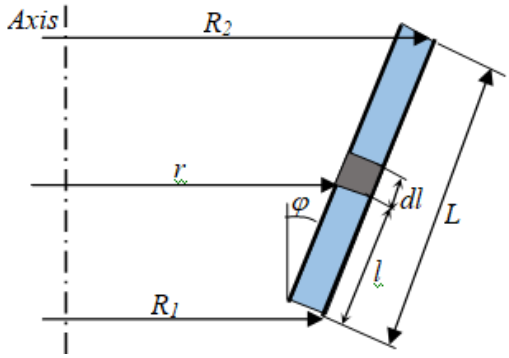

Fig. 3. The ring element of MR fluid in the inclined duct

Plug Eq. (2) into Eq. (1), then take integration along the duct, the following equation can be obtained

$$\begin{aligned} T_I &= 2\pi \int_0^L (R_1 + l\sin\varphi)^2 \left(\tau_y + \mu \frac{\delta\omega\,(R_1 + l\sin\varphi)}{d}\right) \mathrm{d}l \\ &= 2\pi L \left(R_1^2 + R_1 L \sin\varphi + \frac{1}{3}L^2 \sin^2\varphi\right)\tau_y \\ &\quad + \frac{1}{2}\pi\mu\frac{L\Delta\omega}{d}\left(4R_1^3 + 6R_1^2 L\sin\varphi + 4R_1 L^2\sin^2\varphi + L^3\sin^3\varphi\right). \end{aligned} \tag{3}$$

Eq. (3) is used for calculation induced torque in an inclined duct of MRF. From Eq. (3), the induced torque in an annular and radial duct (end-face duct) can be retrieved respectively with $\varphi = 0$ and $\varphi = 90$ degrees, which were widely used in many researches [9, 10] as followings

$$T_a = 2\pi R_a^2 L_a \left(\tau_y + \mu\frac{\Delta\Omega R_a}{d}\right), \tag{4}$$

$$T_E = \frac{\pi\mu_e R_o^4}{2d}\left(1 - \left(\frac{R_i}{R_o}\right)^4\right)\Delta\Omega + \frac{2\pi\tau_y}{3}\left(R_o^3 - R_i^3\right), \tag{5}$$

where T_a is the friction torque of MRF in the annular duct acting on the cylindrical face of the disc, L_a and R_a are respectively the length and the radius of the annular duct, T_e is the friction torque of MRF in the end-face duct acting on the end-face of the disc, R_i and R_o are respectively the inner and outer radius of the end-face duct.

By applying Eqs. (3), (4) and (5) for the MRF ducts of the proposed MRC as shown on Fig. 3 and neglecting of friction due to the sealing and bearings, the induced transmitted

torque can be determined by

$$T_b = 2\left(\sum_{i=1,3,5,7,9} T_{Ii} + \sum_{j=0,2,4,6,8,10} T_{Ej}\right) + T_c, \tag{6}$$

where

$$T_{Ii} = 2\pi l\left(R_i^2 + R_i l sin\phi + \frac{1}{3}l^2 sin^2\phi\right)\tau_{yIi} + \frac{1}{2}\pi\mu_{Ii}\frac{l\Delta\omega}{d}\left(4R_i^3 + 6R_i^2 l sin\phi + 4R_i l^2 sin^2\phi + l^3 sin^3\phi\right), \tag{7}$$

$$T_{Ej} = \frac{\pi\mu_{Ej}R_{j+1}^4}{2d}\left(1 - \left(\frac{R_j}{R_{j+1}^4}\right)^4\right)\Delta\Omega + \frac{2\pi\tau_{yEj}}{3}\left(R_{j+1}^3 - R_j^3\right), \tag{8}$$

$$T_c = 2\pi R_{11}^2(b + 2h)\tau_{yc} + \mu_c\frac{\Delta\Omega R_{11}}{d}, \tag{9}$$

In the above, T_{Ej} is the friction torque induced by MRF in the duct E_j, T_{Ii} is the friction torque induced by MRF in the duct I_i, T_c is the friction torque due to MRF in the cylindrical duct C, R_i is the radius of point i shown in Fig. 4, l and ϕ are respectively the length and angle of the inclined duct, h is the tooth height, τ_{Ei}, τ_{Ii} and τ_c respectively are the yield stress of the MRF in the E_i, I_i and C ducts, μ_{Ei}, μ_{Ii} and μ_c are the post-yield viscosity of the MRF in the E_i, I_i and C ducts respectively.

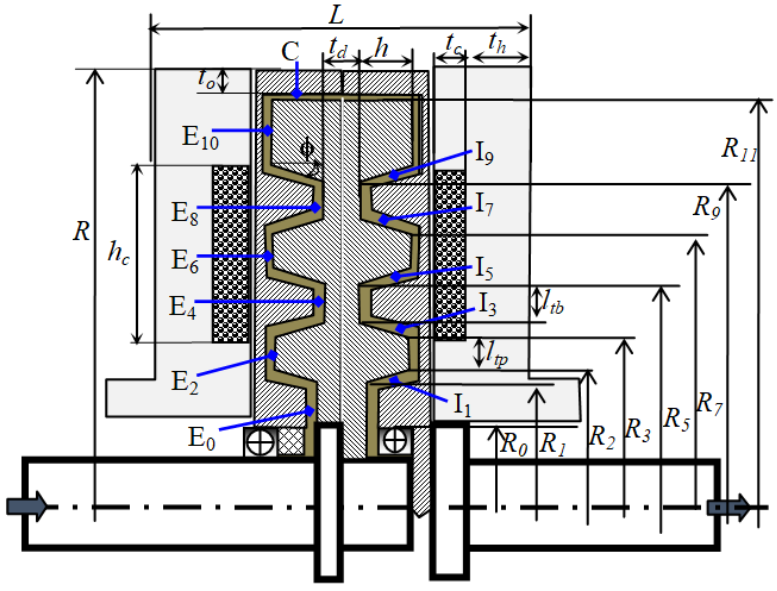

Fig. 4. Illustration of MRF ducts for evaluating transmitted torque

It is noted that the transmitted torque of the conventional MRC [3] is determined by

$$T_{bc} = \frac{\pi\mu R_{do}^4}{d}\left(1 - \left(\frac{R_{di}}{R_{do}}\right)^4\right)\Delta\Omega + \frac{4\pi\tau_{ye}}{3}\left(R_{do}^3 - R_{di}^3\right) + 2\pi R_{do}^2 t_d\left(\tau_{y0} + \mu\frac{\Delta\Omega R_{do}}{d}\right), \tag{10}$$

where R_{di} and R_{do} are the inner and outer radius of the disc, d is the MRF gap size, t_d is the thickness of the disc, τ_{ye} is the average yield stress of MRF in the in the end-face ducts of the MRC, τ_{y0} is the zero-field yield stress and μ is post-yield viscosity of the MRF

3. OPTIMAL DESIGN OF THE MR CLUTCH

In this study, the optimization of the MRC is stated as following: Find optimized value of geometric dimensions of the clutch structure in order to archive a required transmitted torque considering the objective to minimize overall volume of the MRC.

The overall volume of the MRC is determined by

$$V_{MRC} = \pi R^2 L, \tag{11}$$

where R is the overall radius of the MRC and L is the overall length of the MRC. The design variables are: the disc thickness t_d, the tooth-height h, the tooth angle ϕ, tooth-peak length l_{tp}, tooth bottom length l_{tb}, the inner disc radius R_{di} (= R_0), radius of first tooth R_1, the outer disc radius R_{do}(= R_{11}), outer housing thickness of the clutch t_o, the winding core thickness t_h, the coil width t_c, the coil height h_c. The MRF gap size is empirically chosen by 0.8 mm. The thickness of the housing wall is set by 1.25 mm in consideration of manufacturing issues. In order to solve the optimization problem of the MRC, the ANSYS commercial software is employed, in which the axisymmetric element (PLANE 13) and the steepest descent algorithm (first order method) are used. In this study, the silicon steel is used for magnetic components of the MRC such as the side housing, the envelope and the disc. As abovementioned, in the optimization, the maximum achievable transmitted torque of the MRC is constrained to be greater than a required torque. Obviously, the higher applied current is, the stronger magnetic field is generated which in turn results in a higher transmitted torque. Therefore, in order to archive the maximum transmitted torque, the maximum working current (depend on the coil gauge size) is applied to the coils. In this research, the 24-gauge copper wire (the coil wires diameter is 0.511 mm, maximum working current is 2.5A) is used. Hence, the applied current used in the optimization process is 2.5A. The commercial MR fluid, MRF132-DG, is used. For comparison purpose, optimization of the conventional MRC with plain cylindrical disc [3] is also conducted.

Fig. 5 shows the optimal solution of the plain disc MRC while Fig. 6 shows that of the proposed tooth-shaped disc MRC. In the optimization, the required transmitted torque is 10 Nm with an accuracy of 2%, the convergence condition is set by 0.1%. In addition, radius of the clutch shaft is chosen by R_s = 6 mm accounting for the strength of the shaft. From the results, it is found that, at the optimum, transmitted torque of the MRCs is almost 10 Nm as constrained and the overall volume of the conventional MRC is 0.295E-3 m^3 while that of the proposed tooth-shaped disc MRC is 0.159E-3 m^3. Thus, the overall volume of the proposed MRC is much improved (almost half). The reasons

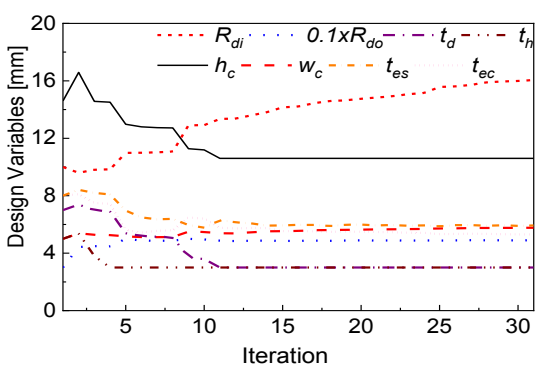

(a) Design variables

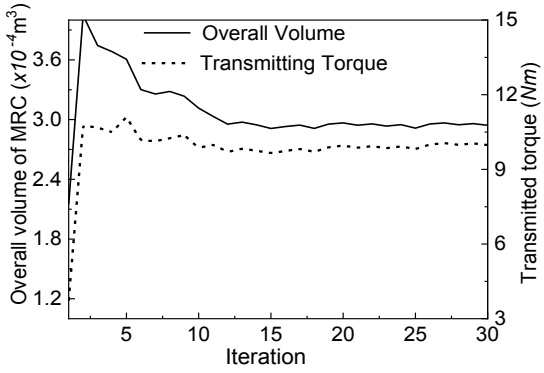

(b) Overall volume and transmitted torque

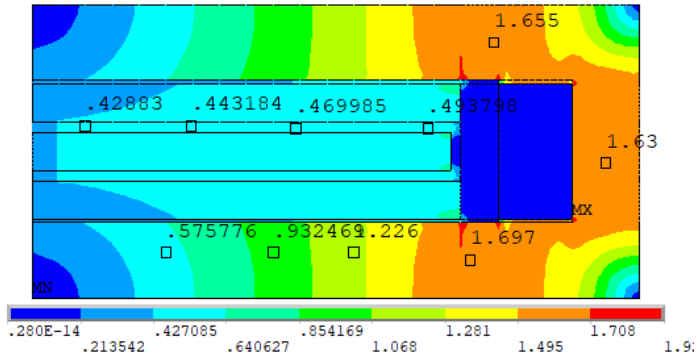

(c) Magnetic density at the optimum

Fig. 5. Optimization solution of the conventional MRC

for this significant volume reduction come from the larger contact area between the rotor and the working MRF and the higher magnetic density across the MRF ducts of the proposed MRC compared to those of the conventional one as shown are shown in Figs. 5(c) and 6(c). The optimal solution is summarized in Table 1. From the table it is also noted that the mass of the proposed MRC is also much smaller than that of the conventional MRC, however, the power consumption of the proposed MRC is almost twice as high as that of the conventional one. This is obvious because in the proposed MRC, two magnetic coils are employed (one on each side) and the power consumption is not considered in the optimization of the MRC. Thus, there is a trade-off between the size and the power consumption of the MRCs. Therefore, in the application where high power is available ant not significant, the proposed MRC can be employed. In order to compromise between the size and the power consumption of the proposed MRC, the power consumption should be taken into account as a constraint function in the optimization. Fig. 7 show the optimal solution of the proposed MRC with the required transmitted torque is 10 Nm and the power consumption is constrained to be smaller than that of the conventional one

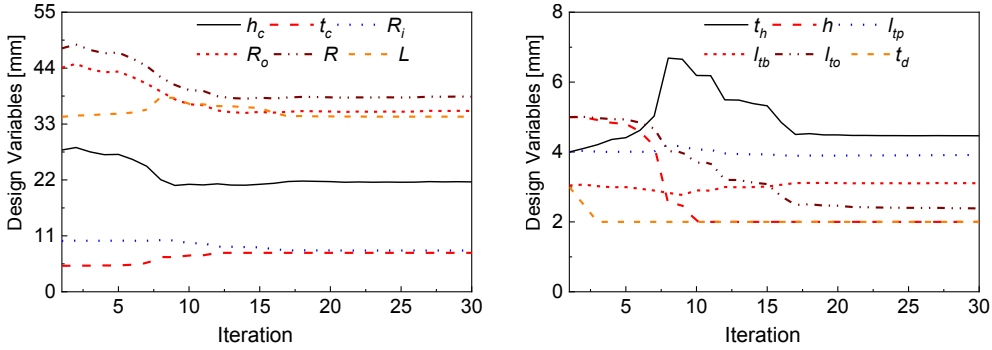

(a) Design variables

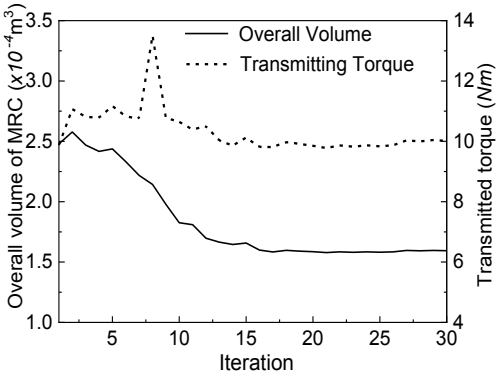

(b) Overall volume and transmitted torque

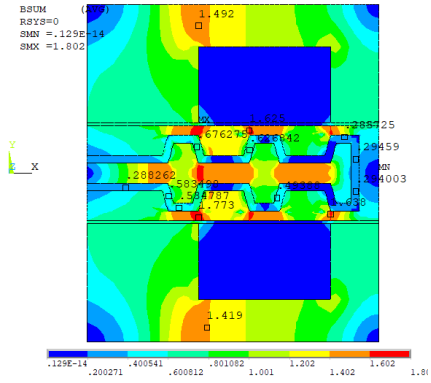

(c) Magnetic density at the optimum

Fig. 6. Optimization solution of the proposed MRC

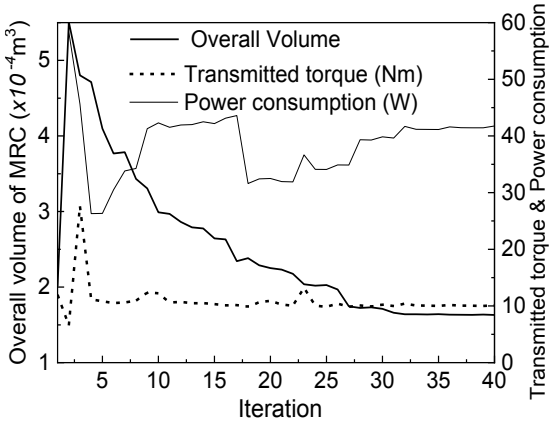

Fig. 7. Optimization solution of the proposed MRC with two constraints: transmitted torque $\geq$ 10 Nm, power consumption $\leq$ 44 W

(44W). It is noted that in this case the applied current is also considered as a design variable. From the figure it is observed that, with the above transmitted torque and power consumption, the overall volume of the proposed MRC is 0.166E-3 m^3, which is still significantly smaller than that of the conventional one (0.295E-3 m^3). It is noteworthy that at the optimum the applied current is 1.77A. From the above, it is remarked that in order to compromise between the size and power consumption of the MRC, the power consumption should be conserved as a constraint function and the applied current should be treated as a design variable.

Table 1. Significant parameters of the optimized MRCs

MRC types	Design parameter (mm)	Characteristics (at I = 2.5A)
Conventional	Coil: width $t_c = 10.6$; height $h_c = 5.75$; No. turns: 238 Housing thickness: side $t_h = 3$, cylindrical $t_o = 3$ Fixed Housing: side $t_{fh} = 5.9$, cylindrical $t_{fo} = 5.3$, overall size $R = 63.8, L = 23.0$ Disc: inner radius $R_{di} = 16.0$, outer radius $R_{do} = 48.9$; thickness $t_d = 3$ MRF duct gap: 0.8	Max. Torque: 10 Nm Overall Volume (m^3): 0.295E-3 Off-state Torque: 0.3 Nm Mass (kg): 2.3 Power Cons.: 44 W Coil Resistance(Ω): $R_c = 7.0$
Proposed	Coil: width $t_c = 7.7$; height $h_c = 21.6$; No. of turns: 2*500 Fixed Housing: thickness $t_h = 4.5$, overall size $R = 38.4, L = 34.5$ Disc: $R_i = 8.0$, $R_d = 36.4$, $t_d = 2.0, h_t = 2.0, l_{tp} = 3.9, l_{tb} = 4.5, l_{to} = 2.5, \phi = 1.07$ rad MRF duct gap: 0.8	Max. Torque: 10 Nm Overall Volume (m^3): 0.159E-3 Mass: 1.24 kg Off-state Torque: 0.293 Nm Power Cons.: 85 W Coil Resistance(Ω): $R_c = 6.8$

In order to investigate performance of the proposed MRC at different maximum transmitted torques, the optimization of the MRCs at different values of the required transmitted torque are conducted and the results are shown in Fig. 8. As shown in Fig. 8(a), the overall volume of the MRCs increases with the required transmitted torque. The overall volume of the proposed MRC is significantly smaller than that of the conventional one with a volume ratio ranging from 60% at the required torque of 5 Nm to 45% at the required torque of 100 Nm. In contrary, the power consumption of the proposed MRC is almost as twice as that of the proposed one at different value of the required torque as shown in Fig. 8(b).

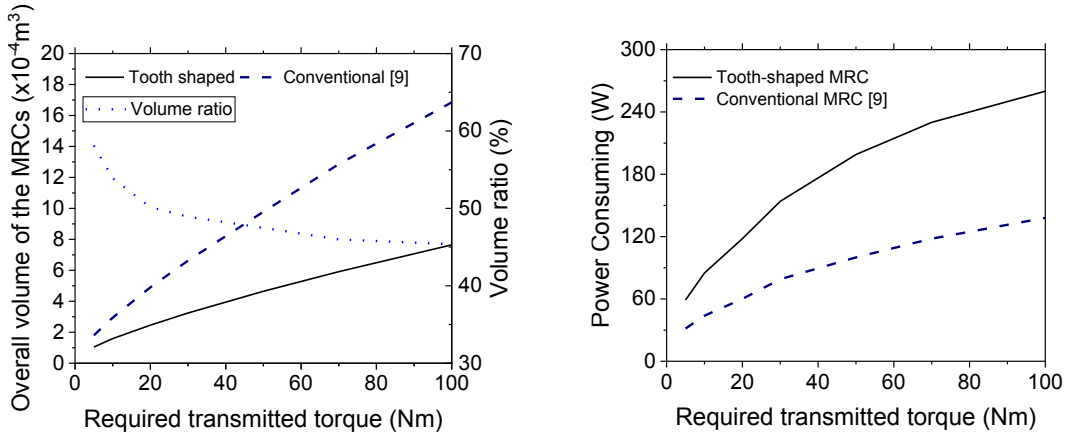

(a) Overall volume (b) Power consumption

Fig. 8. Optimal results of the MRCs as different values of the required transmitted torque

4. EXPERIMENTAL VALIDATION

In this part, the above optimized MRC is fabricated and its performance characteristics are tested by experimental works. Fig. 9 shows experiment apparatus to evaluate transmitted torque of the MRC. The 500W-DC servo motor with gearbox is controlled by a computer to constantly rotate at 300 rpm, the output shaft of the motor is connected to the input shaft of the MRC while the output shaft of the MRC is connected to an stationary torque sensor. When the experimental process is commenced, a step current with different magnitude (0.5A, 0.75A, 1.0A, 1.25A, 1.5A, 1.75A, 2.0A, 2.5A) is applied to the two coils of the MRC and the transmitted torque is measured by the torque sensor.

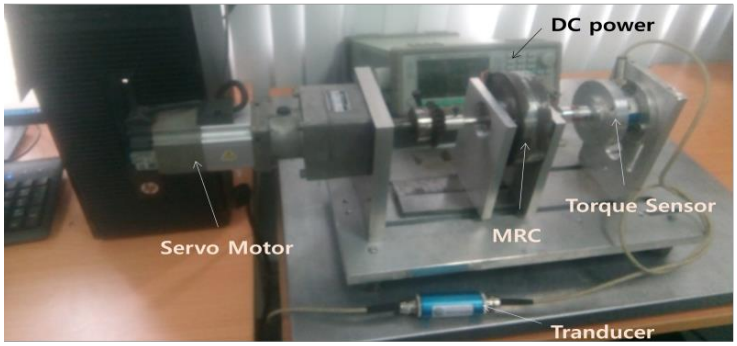

Fig. 9. Experiment apparatus to test the proposed MRC

Fig. 10 show the results obtained from experiments. From Fig. 10(a), it is observed that the measured transmitted torque at the applied current of 2.5A is around 10.4 Nm, which is a bit greater than that of the simulation (9.9 Nm). The main reason may come

from the neglecting of the friction torque of the sealing and bearings in simulated results. It is also observed from Fig. 10(b) that at different applied currents, different values of output torque can be archived and very closed to the simulated ones; the error is within 5%. It is also found the torque response time is around 0.25 s, which is very good time response for application in industry.

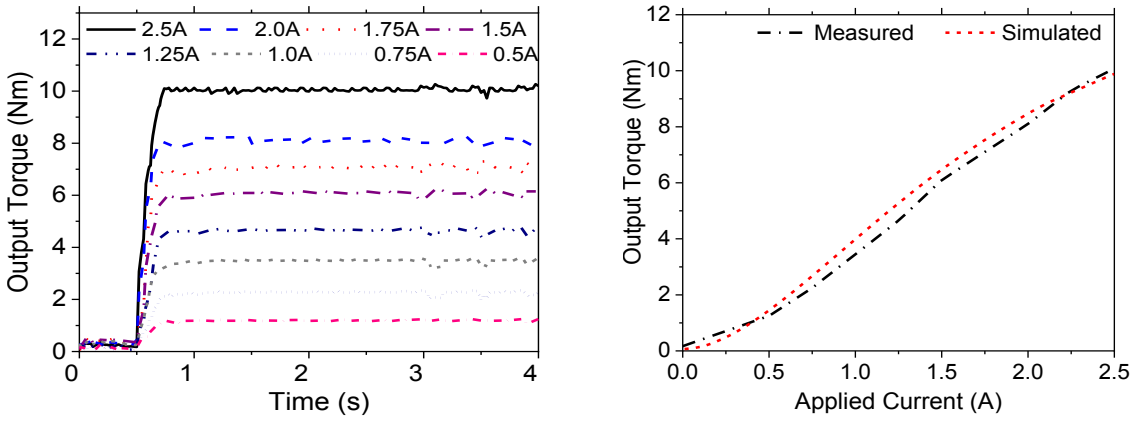

(a) Measured torque

(b) Simulated vs. measured torque

Fig. 10. Experiment results of step response of the MRC

5. CONCLUSIONS

In this study, a novel configuration of magneto-rheological clutch (MRC) featuring a tooth shaped disc was proposed. The inner face of the clutch housing also has tooth shaped features mating with the teeth of the disc via MRF layer. Excitation magnetic coils are assembled on stationary winding cores placed on both side of the clutch housing. An air gap of 0.3 mm is left between the housing and the winding cores to ensure the housing can freely rotate against the winding cores. Optimal design of the proposed MRC considering transmitted torque and overall volume of the MRC was conducted and compared with traditional MRC featuring plain cylindrical disc. The optimal results showed that at the same required transmitted torque, the overall volume and mass of the proposed MRC are significantly smaller than those of the conventional one (almost half). However, the power consumption of the proposed MRC is around double of the conventional one because two coils are implemented. In order to compromise between the size and the power consumption of the proposed MRC, the optimization with two constraints (transmitted torque and power consumption) and was conducted. The results showed that with the power consumption is constrained to be smaller than the power consumption of the conventional one, the overall mass of the MRC is still significantly smaller than that of the conventional one. The optimized MRC was then manufactured for testing. Experimental works showed a good agreement between the measured transmitted torque and the simulated one.

ACKNOWLEDGEMENT

This work was supported by the Vietnam National Foundation for Science and Technology Development (NAFOSTED) under grant number 107.01-2018.335.

REFERENCES

[1] J. Wang and G. Meng. Magnetorheological fluid devices: Principles, characteristics and applications in mechanical engineering. *Proceedings of the Institution of Mechanical Engineers, Part L: Journal of Materials: Design and Applications*, **215**, (2001), pp. 165–174. https://doi.org/10.1243/1464420011545012.

[2] A. Muhammad, X. liang Yao, and Z. chao Deng. Review of magnetorheological (MR) fluids and its applications in vibration control. *Journal of Marine Science and Application*, **5**, (2006), pp. 17–29. https://doi.org/10.1007/s11804-006-0010-2.

[3] T. D. Truong, V. Q. Nguyen, B. T. Diep, D. H. Q. Le, D. T. Le, and Q. H. Nguyen. Speed control of rotary shaft at different loading torque using MR clutch. In A. Erturk, editor, *Active and Passive Smart Structures and Integrated Systems XIII*, SPIE, (2019), https://doi.org/10.1117/12.2515309.

[4] U. Lee, D. Kim, N. Hur, and D. Jeon. Design Analysis and Experimental Evaluation of an MR Fluid Clutch. *Journal of Intelligent Material Systems and Structures*, **10**, (1999), pp. 701–707. https://doi.org/10.1106/ex6x-y4qq-xq5l-8jjv.

[5] T. Kikuchi, K. Ikeda, K. Otsuki, T. Kakehashi, and J. Furusho. Compact MR fluid clutch device for human-friendly actuator. *Journal of Physics: Conference Series*, **149**, (2009). https://doi.org/10.1088/1742-6596/149/1/012059.

[6] D. Wang and Y. Hou. Design and experimental evaluation of a multidisk magnetorheological fluid actuator. *Journal of Intelligent Material Systems and Structures*, **24**, (2012), pp. 640–650. https://doi.org/10.1177/1045389x12470305.

[7] K. H. Latha, P. U. Sri, and N. Seetharamaiah. Design and Manufacturing Aspects of Magnetorheological Fluid (MRF) Clutch. *Materials Today: Proceedings*, **4**, (2), (2017), pp. 1525–1534. https://doi.org/10.1016/j.matpr.2017.01.175.

[8] Q. H. Nguyen and S.-B. Choi. A new method for speed control of a DC motor using magnetorheological clutch. In *Active and Passive Smart Structures and Integrated Systems 2014*, International Society for Optics and Photonics, (2014), https://doi.org/10.1117/12.2044558.

[9] Q. H. Nguyen, N. D. Nguyen, and S. B. Choi. Design and evaluation of a novel magnetorheological brake with coils placed on the side housings. *Smart Materials and Structures*, **24**, (2015). https://doi.org/10.1088/0964-1726/24/4/047001.

[10] N. D. Nguyen, T. Le-Duc, L. D. Hiep, and Q. H. Nguyen. Development of a new magnetorheological fluid–based brake with multiple coils placed on the side housings. *Journal of Intelligent Material Systems and Structures*, **30**, (2018), pp. 734–748. https://doi.org/10.1177/1045389x18818385.